Mechanism of drug extrusion by brain endothelial cells via lysosomal drug trapping and disposal by neutrophils

Andreas Noack[a,1], Birthe Gericke[a,1], Maren von Köckritz-Blickwede[b,c], Arne Menze[a], Sandra Noack[d], Ingo Gerhauser[e], Felix Osten[a], Hassan Y. Naim[b,2], and Wolfgang Löscher[a,f,2,3]

[a]Department of Pharmacology, Toxicology, and Pharmacy, University of Veterinary Medicine Hannover, 30559 Hannover, Germany; [b]Department of Physiological Chemistry, University of Veterinary Medicine Hannover, 30559 Hannover, Germany; [c]Research Center for Emerging Infections and Zoonoses, University of Veterinary Medicine Hannover, 30559 Hannover, Germany; [d]Department of Trauma Surgery, Hannover Medical School, 30625 Hannover, Germany; [e]Department of Pathology, University of Veterinary Medicine Hannover, 30559 Hannover, Germany; and [f]Center for Systems Neuroscience, 30559 Hannover, Germany

Edited by Solomon H. Snyder, Johns Hopkins University School of Medicine, Baltimore, MD, and approved August 31, 2018 (received for review November 10, 2017)

The blood–brain barrier protects the brain against a variety of potentially toxic compounds. Barrier function results from tight junctions between brain capillary endothelial cells and high expression of active efflux transporters, including P-glycoprotein (Pgp), at the apical membrane of these cells. In addition to actively transporting drugs out of the cell, Pgp mediates lysosomal sequestration of chemotherapeutic drugs in cancer cells, thus contributing to drug resistance. Here, we describe that lysosomal sequestration of Pgp substrates, including doxorubicin, also occurs in human and porcine brain endothelial cells that form the blood–brain barrier. This is followed by shedding of drug-sequestering vesicular structures, which stay attached to the apical side of the plasma membrane and form aggregates ("barrier bodies") that ultimately undergo phagocytosis by neutrophils, thus constituting an as-yet-undescribed mechanism of drug disposal. These findings introduce a mechanism that might contribute to brain protection against potentially toxic xenobiotics, including therapeutically important chemotherapeutic drugs.

blood–brain barrier | P-glycoprotein | doxorubicin | lysosomes | neutrophils

The blood–brain barrier (BBB) controls the entry of compounds into the brain, thereby regulating brain homeostasis (1). ATP-binding cassette (ABC) multidrug efflux transporters such as P-glycoprotein (Pgp; MDR1; ABCB1) are expressed at the apical membrane of brain capillary endothelial cells (BCECs) that form the BBB. These transporters significantly contribute to BBB function by limiting brain entry of potentially cytotoxic compounds via active efflux of such compounds to the blood (2–4). Pgp is synthesized in the endoplasmic reticulum and trafficked along the secretory pathway through the Golgi apparatus to the cell surface, but is also localized to endosomes and lysosomes (5). The localization of Pgp in endosomes has been suggested to serve as an intracellular reservoir before Pgp moving to the plasma membrane, while lysosomes are responsible for Pgp degradation (5). However, data obtained in cancer cells have indicated that Pgp is also expressed in the lysosomal membrane and can sequester ionizable chemotherapeutics such as doxorubicin (DOXO) into lysosomes to prevent interaction with molecular targets, resulting in drug resistance (6–11). This lysosomal drug sequestration is enabled by the topological inversion of Pgp via endocytosis, resulting in the transporter actively pumping agents into the lysosome (12, 13). Consequently, lysosomal drug sequestration is prevented by Pgp inhibitors such as valspodar and elacridar or silencing Pgp expression with siRNA (9). Lysosomal trapping of Pgp substrates and its inhibition by Pgp inhibitors has not only been demonstrated for cancer cell lines but also for lysosome-rich organs (kidney and spleen) of healthy humans (14). However, it is not known whether similar Pgp-mediated lysosomal drug sequestration is also functional in BCECs that form the BBB, thus contributing to BBB function.

We recently described intercellular Pgp transfer in human brain endothelial (hCMEC/D3) cells using cocultures of wild-type (WT) and Pgp-EGFP–expressing cells (15). In subsequent experiments in such confluent cocultures, which are described in the present work, we observed the intracellular formation of Pgp substrate [eFluxx-ID Gold (EFIG)]– and Pgp-EGFP–containing vesicular structures and subsequent shedding of these Pgp-substrate–sequestering vesicular structures. These structures stayed attached to the apical side of the plasma membrane and formed aggregates, which we termed "barrier bodies." To our knowledge, such membrane-attached Pgp/substrate sequestering structures have not been described for BCECs or any other Pgp-containing cell type. The extracellular localization of these structures and their attachment to the apical cell membrane of the BCECs led us to hypothesize that the formation and shedding

Significance

Located at the apical (blood-facing) site of brain capillary endothelial cells that form the blood–brain barrier (BBB), the efflux transporter P-glycoprotein (Pgp) restricts the brain entry of various lipophilic xenobiotics, which contributes to BBB function. Pgp may become saturated if exposed to too-high drug concentrations. Here, we demonstrate a second-line defense mechanism in human brain capillary endothelial cells—that is, Pgp-mediated intracellular lysosomal drug trapping. Furthermore, we describe a mechanism of drug disposal at the BBB, which is shedding of lysosomal Pgp/substrate complexes at the apical membrane of human and porcine BBB endothelial cells and subsequent phagocytosis by neutrophils. Thus, we have discovered a fascinating mechanism of how Pgp might contribute to brain protection.

Author contributions: A.N., B.G., M.v.K.-B., H.Y.N., and W.L. designed research; A.N., B.G., A.M., S.N., I.G., and F.O. performed research; A.N., B.G., A.M., S.N., I.G., and F.O. analyzed data; and A.N., B.G., M.v.K.-B., H.Y.N., and W.L. wrote the paper.

The authors declare no conflict of interest.

This article is a PNAS Direct Submission.

[1]A.N. and B.G. contributed equally to this work.

[2]H.Y.N. and W.L. contributed equally to this work.

[3]To whom correspondence should be addressed. Email: wolfgang.loescher@tiho-hannover.de.

This article contains supporting information online at www.pnas.org/lookup/suppl/doi:10.1073/pnas.1719642115/-/DCSupplemental.

Published online September 25, 2018.

of the barrier bodies may be an effective way for the cell to dispose of cytotoxic compounds via phagocytic blood cells and, thus, provide a second-line defense mechanism against cytotoxic drugs. The present findings support this hypothesis.

Results

First Observation of Barrier Bodies. During a series of live cell imaging experiments on intercellular Pgp transfer in confluent cocultures of equal numbers of hCMEC/D3 WT cells (Pgp-recipient cells) and conditional doxycycline-inducible Pgp-EGFP–overexpressing hCMEC/D3 cells (Pgp-donor cells), we used EFIG, a xanthene-based small-molecule dye coupled to acetoxymethyl (AM) ester (EFIG-AM) for cell permeability (16). EFIG has been optimized for multiplexing with other common fluorescent dyes in cell imaging and flow-cytometric assays, allowing the concomitant use of several dyes as done in this study (16). The nonfluorescent proprietary AM-ester form of EFIG readily penetrates the cell membrane due to its hydrophobic character and is subsequently hydrolyzed by intracellular esterases (16). Cleavage by esterases results in a hydrophilic cell membrane-impermeable fluorescent metabolite of EFIG-AM, EFIG, which is trapped inside the cell unless it is pumped out by efflux transporters like Pgp (16). The fluorescence signal of the dye generated within the cells thus depends upon the activity of such efflux transporters (15, 17). In Pgp-EGFP–overexpressing hCMEC/D3 cells, EFIG efflux is almost completely inhibited when cells are treated with specific Pgp inhibitors (15, 18).

When the coculture was exposed to EFIG-AM in live cell imaging experiments, data from confocal fluorescence microscopy showed that the cytoplasm of eFluor670 (APC)-labeled WT cells appeared red-colored (arrow 1 in Fig. 1), because the esterase-cleaved fluorescent dye EFIG was trapped inside the cells. In contrast, hCMEC/D3 donor cells overexpressing Pgp-EGFP in their plasma membrane did not appear red (arrow 2 in Fig. 1), because the esterase-cleaved dye EFIG was effectively pumped out of the cells by Pgp. As recently shown (15), in such cocultures of hCMEC/D3 WT cells and Pgp-EGFP–overexpressing hCMEC/D3 cells, the Pgp-EGFP fusion protein is transferred from donor to recipient cells by cell-to-cell contact and Pgp-EGFP–enriched vesicles, which are exocytosed by donor cells and endocytosed by adjacent recipient cells. WT cells that received Pgp-EGFP by such intercellular transfer also did not appear red in response to EFIG-AM exposure (arrow 3 in Fig. 1).

In addition to efflux of the fluorescent EFIG out of the cells [which we demonstrated in previous experiments with these cells (15, 18)], we observed the intracellular formation of Pgp substrate (EFIG) and Pgp-EGFP–containing vesicular structures (~0.5–2 μm in diameter) that were either formed in the Pgp-EGFP–expressing endothelial cells (arrow 4 in Fig. 1) or, after intercellular transfer of Pgp-EGFP, in eFluor670-labeled WT cells (arrow 5 in Fig. 1). The Pgp-EGFP/substrate–containing vesicular structures were shed by the endothelial cells and formed extracellular aggregates with an aciniform structure and a size of 5–25 μm in diameter (arrow 6 in Fig. 1). Both hCMEC/D3 WT and Pgp-EGFP–overexpressing hCMEC/D3 cells formed these vesicular aggregates, which stayed attached to the plasma membrane. We therefore termed these aciniform large structures barrier bodies, because they attached to the blood-facing apical plasma membrane of BCECs that form the BBB (see description of experiments in two-compartment chamber devices below).

To confirm the extracellular localization of these aggregates, confocal optical sectioning of cocultured hCMEC/D3 cells treated with EFIG-AM was performed. Structures identified as barrier bodies in a maximum projection image from a stack of 40 optical sections (*SI Appendix*, Fig. S1*A*, white circles) could be associated with elevated areas in a 3D image, by using depth coding (*SI Appendix*, Fig. S1*B*, white circles). In depth-coding images, different focal planes were represented by a color code. The same

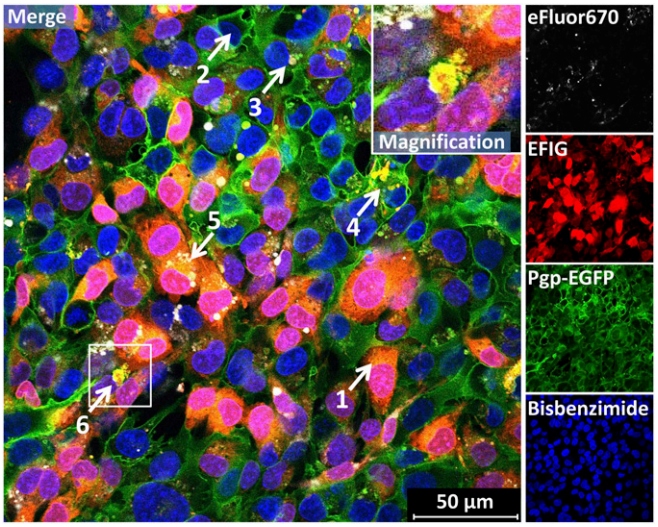

Fig. 1. Formation of intracellular and extracellular Pgp/EFIG-enriched vesicles by BCECs. hCMEC/D3-MDR1-EGFP (Pgp donor) and hCMEC/D3 WT (Pgp recipient) cells were cocultured on coverslips (*Materials and Methods*). Live cell imaging was performed by confocal fluorescence microscopy. WT cells can be identified by eFluor670 fluorescence labeling (white), performed before seeding. Three days after confluence, cells were treated with EFIG-AM (30 min) and afterward analyzed by live cell confocal microscopy. The hydrophobic nonfluorescent EFIG-AM readily penetrates the cell membrane and is subsequently hydrolyzed by intracellular esterases to the hydrophilic fluorescent dye EFIG (red), which localizes in the cytoplasm of WT cells (1) but not in that of Pgp-EGFP–overexpressing (green) cells (2) or WT cells with transferred Pgp from neighboring donor cells (3). Pgp and EFIG colocalize in intracellular vesicular structures in MDR1-EGFP (4) and WT cells (5). Aggregates of Pgp/EFIG-enriched vesicles (barrier bodies) at the plasma membrane borders of different cells (6). (*Inset*) White frame in merged image outlines the section magnified in the upper right corner. Cell nuclei are stained by bisbenzimide H (blue).

structures revealed a superimposed localization on the cells, when the cell layer was analyzed for its 3D architecture (*SI Appendix*, Fig. S1*C*, white arrow).

Barrier Bodies Are also Formed with DOXO. To examine whether the observed intracellular sequestration of Pgp substrate and extracellular formation of barrier bodies only occurred with the Pgp substrate EFIG or also with more widely used cytotoxic Pgp substrates, we performed similar live cell imaging experiments with DOXO at subtoxic concentrations (10 μM). DOXO is one of the most widely used clinical anticancer agents and a hydrophobic weak base that intercalates as primary target into nuclear DNA (19). When cocultures of hCMEC/D3 WT cells and Pgp-EGFP–overexpressing hCMEC/D3 cells were exposed to DOXO (10 μM, 30 min), nuclear binding of DOXO (red) was only observed in WT cells not overexpressing Pgp (Figs. 2 and 3*D*). The data obtained with EFIG were corroborated by similar observations in DOXO-exposed cells. First, after treatment with DOXO, Pgp-EGFP–transfected hCMEC/D3 cells showed an intracellular sequestration of DOXO in Pgp-containing vesicles, located within the cytoplasm near the cell nuclei (arrows labeled 1 in Fig. 2); similarly, WT cells showed accumulation of DOXO in intracellular vesicular structures (arrow 2 in Fig. 2). Second, in addition to intracellular localization of Pgp/DOXO-containing vesicles, confocal microscopic analysis showed an assembly of Pgp/DOXO-positive vesicles (with the same features as the barrier bodies first observed with EFIG) at the plasma membrane border of different cells (arrows labeled 3 in Fig. 2). Notably, most of the barrier-body aggregates, either formed after DOXO or EFIG-AM treatment of hCMEC/D3 cells, seemed to

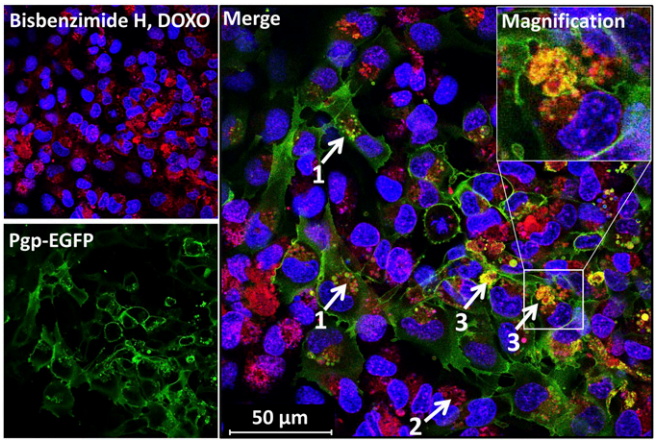

Fig. 2. Intracellular Pgp/Pgp substrate vesicle and barrier-body formation after exposure of BCECs to DOXO. Cocultured hCMEC/D3-MDR1-EGFP and hCMEC/D3 WT cells were treated with DOXO (10 µM, 30 min) and subsequently analyzed by live cell imaging and confocal microscopy. DOXO (red) is enriched in Pgp-EGFP positive (green) intracellular vesicles of EGFP-overexpressing cells (1). Likewise, DOXO accumulates in vesicular structures near to cell nuclei of WT cells (no green fluorescence) (2). Like the results from EFIG-AM treatment of hCMEC/D3 cells, accumulation of Pgp/DOXO-enriched vesicles (barrier bodies) can be observed at the plasma membrane borders of the cells (3). (*Inset*) Magnification of barrier body (white frame, merged image). For orientation, cell nuclei were stained by the DNA intercalating dye bisbenzimide H (blue).

be enclosed by a Pgp-containing membrane, most likely due to budding from the hCMEC/D3 plasma membrane (*Insets* in Figs. 1 and 2). Analysis of the number of barrier bodies in 10 randomly captured fluorescent micrographs of different cultures treated with either DOXO ($n = 4$) or EFIG-AM ($n = 6$) showed that 135 of 1,323 analyzed cells (10.2%) exhibited barrier-body aggregates (range 8.1–13.9% per image) without significant difference between treatments.

Scanning electron microscopy was used to analyze the structure of barrier bodies and their extracellular formation at higher resolution. Fig. 4*A* illustrates the budding of vesicles (1–2 µm in diameter) from the apical membrane of hCMEC/D3 cells after treatment with DOXO. Fig. 4*B* shows the accumulation of the extracellular vesicles (EVs) in aciniform aggregates at the apical cell surface of hCMEC/D3 cells, similar to the structure of the barrier bodies seen with laser scanning microscopy.

Intracellular Sequestration of Pgp Substrates in Vesicular Structures Positive for Lysosomal Markers. It has been demonstrated in cancer cells that Pgp not only functions to transport drugs out of the cell when present on the plasma membrane, but also adopts a role in the lysosomal membrane to induce resistance (13). This mechanism is enabled by the topological inversion of Pgp via endocytosis, resulting in the transporter actively pumping agents into the lysosome (12). Lysosomes thus act as a "safe house" to prevent cytotoxic effects of Pgp substrates that have surpassed the efflux of the plasma membrane-located Pgp (9, 11–13). We therefore thought that the same mechanism of Pgp substrate sequestration is active in BCECs. Indeed, the intracellular structures that sequestered the Pgp substrates EFIG and DOXO in hCMEC/D3 cells were identified as lysosomes by LAMP-2 and LysoTracker staining and confocal microscopy (Fig. 3). Absent binding of DOXO to its primary nuclear target in Pgp-EGFP–overexpressing cells (arrow 1 in Fig. 3*D*) in comparison with WT cells with lower levels of Pgp (arrow 2 in Fig. 3*D*) is due to entrapment of DOXO in lysosomes or active transport out of the cell by Pgp within the plasma membrane. A double staining of intracellular Pgp/Pgp substrate vesicles and lysosomal markers LAMP-2 or LysoTracker is shown in *SI Appendix*, Fig. S2.

Barrier Bodies also Contain Lysosomal Markers. For live cell imaging of cocultured WT and Pgp-EGFP–overexpressing hCMEC/D3 cells, lysosomes were visualized by incubation with LysoTracker before treatment with Pgp substrate (Fig. 5). The extracellular barrier bodies showed LysoTracker staining indicating an endo-lysosomal origin of these structures. Interestingly, the diameter of single vesicles in the barrier bodies lies in a range of 0.5–2 µm, which is similar to the diameter of lysosomes, but exceeds the diameter of exosomes or ectosomes so far described (20, 21). A prestaining of nuclear DNA (DAPI, bisbenzimide H; blue) before Pgp substrate treatment of hCMEC/D3 cells and an absent DAPI staining of the formed barrier bodies suggest that shedding of barrier bodies does not result from apoptotic events (magnified images in Figs. 1 and 2). Apoptosis of hCMEC/D3 cocultures after substrate treatment was additionally examined in Western blots from cell lysates, analyzing cleavage of caspase-3 (*SI Appendix*, Fig. S3*F*). Neither in cocultures treated with DOXO (10 µM, 30 min) nor with EFIG-AM (30 min) was caspase-3 cleavage as marker for apoptosis detectable.

In subsequent experiments, barrier bodies were isolated from cocultured hCMEC/D3 cells treated with Pgp substrate by using differential centrifugation and FACS analysis to assess bisbenzimide

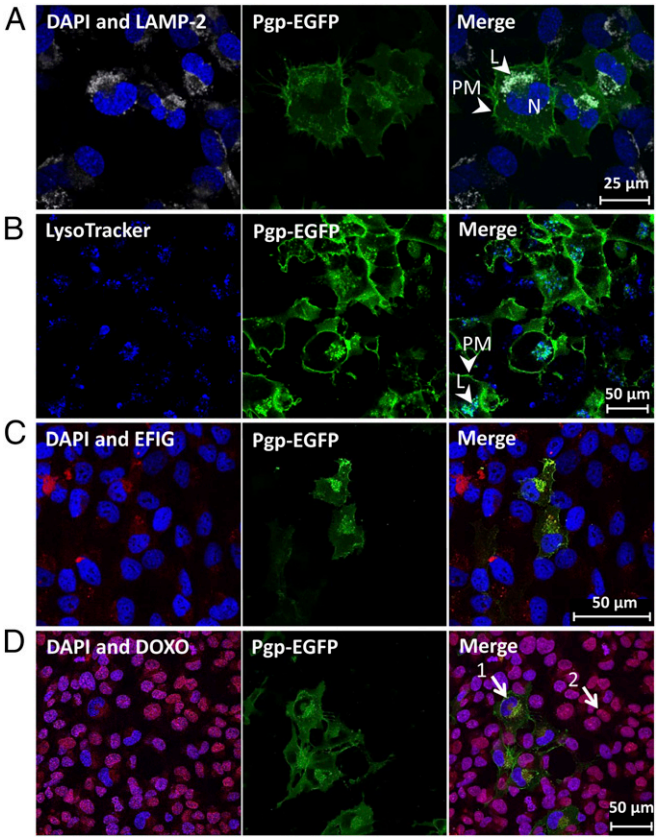

Fig. 3. Sequestration of Pgp substrate into Pgp-enriched lysosomes of BCECs. (*A* and *B*) Intracellular Pgp-EGFP– enriched (green) structures in hCMEC/D3 cells were identified as lysosomes by staining for lysosomal marker LAMP-2 (gray) in paraformaldehyde-fixed cells (*A*) and with LysoTracker staining (75 nM, 1 h) (blue) in live cell imaging (*B*). (*C* and *D*) Pgp substrate sequestration into Pgp-enriched lysosomes is shown after treatment with EFIG-AM (*C*) and DOXO (*D*) individually. DAPI was used as nuclear counterstain (blue). Samples were analyzed by confocal fluorescence microscopy. L, lysosome; N, nucleus; PM, plasma membrane.

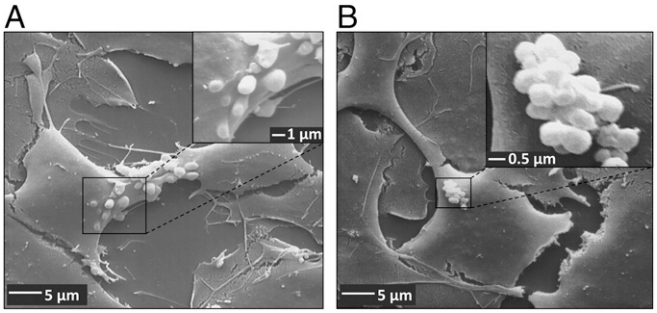

Fig. 4. Vesicle formation and aggregation at the apical surface of human BCECs after treatment with DOXO. hCMEC/D3 cocultures were grown on collagen-coated coverslips in 24-well cell culture plates. After treatment with DOXO (10 µM, 30 min), cocultures were fixed with 2.5% glutaraldehyde for analysis by scanning electron microscopy. (*A*) A scanning electron micrograph showing vesicle formation at the apical plasma membrane of hCMEC/D3 cells after treatment with DOXO. Vesicle size in diameter: 1–2 µm. [Magnification: 2,000× (main image) and 10,000× (*Inset*).] (*B*) Representative scanning electron micrograph showing aggregation of EVs at the apical surface of hCMEC/D3 cells, thus forming aciniform barrier bodies. The single vesicle size in diameter ranged from 0.6 to 2 µm, and the size of EV aggregates in diameter ranged from 5 to 16 µm. [Magnification: 2,000× (main image) and 20,000× (*Inset*).]

H-negative and Pgp/Pgp substrate-positive vesicular structures (for details see *SI Appendix*, *SI Materials and Methods* and Fig. S3 *A–D*). Dot blotting of the isolated bodies revealed localization of LAMP-2 within barrier bodies (*SI Appendix*, Fig. S3*E*), thus supporting the hypothesis that barrier bodies are of lysosomal origin. Moreover, the small GTPase binding protein Rho A and the lipid raft marker flotillin-2 were detected in barrier-body isolates. FACS analysis additionally unraveled that 58% of the barrier bodies originate from Pgp-EGFP–overexpressing cells and 42% from eFluor670-labeled WT cells, to which Pgp was transferred (*SI Appendix*, Fig. S3*C*).

The localization of barrier-body aggregates at the plasma-membrane border of adjacent cells (Figs. 1 and 2) and the presence of both the WT marker eFluor670 and Pgp-EGFP in the barrier bodies (Fig. 1 and *SI Appendix*, Fig. S3*C*) indicated that each barrier-body aggregate (which was exhibited by ∼10% of the cells) was formed by vesicles from more than one endothelial cell. This suggests that at least 20% of the cells in the cocultures contributed to barrier-body formation.

Barrier-Body Formation Is Blocked by Inhibition of Vesicular Trafficking and Reduced by Inhibition of Pgp. Vesicular trafficking to the cell surface implicates particularly the actin cytoskeleton and the microtubules (22, 23). We therefore asked whether the entire process of barrier-body formation can be blocked by nocodazole, which interferes with the polymerization of microtubules (24, 25), or cytochalasin D, which is a cell-permeable and potent inhibitor of actin polymerization (26). As shown in Fig. 6, both nocodazole (10 µM) and cytochalasin D (10 µM) markedly (∼90%) reduced the formation of barrier bodies, but did not affect cell viability. It is noteworthy that inhibition of Pgp by elacridar (0.2 µM) significantly reduced barrier-body formation by 51% on average (Fig. 6*C*).

Barrier Bodies Are Eliminated by Phagocytosing Neutrophils. The extracellular localization of these structures and their attachment to the blood-facing apical cell membrane of the BCECs led us to hypothesize that the formation of the barrier bodies may constitute an efficient cellular mechanism for the disposition of cytotoxic compounds to phagocytic blood cells. Two strategies were used to evaluate this hypothesis: (*i*) incubation of human promyelocytic HL-60 cells, which can be chemically induced to differentiate to a neutrophil-like phenotype (27), with isolated single barrier-body vesicles; and (*ii*) coculturing of WT and EGFP-Pgp–transfected hCMEC/D3 cells with human primary blood-derived neutrophils.

HL-60 cells were differentiated to a neutrophil-like cell type by DMSO treatment and incubated with the Pgp/Pgp substrate-positive barrier bodies isolated by differential centrifugation and FACS analysis. Interestingly, a perinuclear localization of the barrier bodies was observed after addition to the HL-60 cells and removal of the barrier bodies from the culture medium by washing (*SI Appendix*, Fig. S4*A*, arrow), providing clear evidence for an uptake of barrier bodies by phagocytosing neutrophil-like HL-60 cells.

For further investigation of a barrier-body uptake by phagocytic blood cells, freshly isolated human blood-derived neutrophils were used. Human neutrophils do not endogenously express Pgp (28, 29); thus, a green fluorescence signal of neutrophils after incubation with Pgp-EGFP–expressing hCMEC/D3 cocultures or barrier bodies would indicate a Pgp uptake by neutrophils. In a first step, human neutrophils were incubated with isolated Pgp/substrate-positive vesicles, and a possible ingestion of the bodies was examined by fluorescence microscopy. A Pgp/Pgp substrate-positive fluorescence staining of the neutrophils indicated that these cells have in fact phagocytosed the barrier body (*SI Appendix*, Fig. S4*B*). Such fluorescence was not seen in negative controls. In a second step, human neutrophils were incubated with cocultured hCMEC/D3 cells pretreated with EFIG-AM and analyzed for Pgp/Pgp-substrate uptake by live cell imaging and fluorescence microscopy (Fig. 7 and Movie S1). During a time course of 32 min after the addition of neutrophils to cocultured hCMEC/D3 cells, the neutrophils showed an increasing fluorescent signal for Pgp-EGFP and Pgp substrate that colocalized in punctate structures (Fig. 7*A*, magnification). The punctate distribution of Pgp/Pgp substrate within the neutrophils indicated an uptake of the barrier-body vesicles. Lysosomes of hCMEC/D3 cells were marked by LysoTracker staining before Pgp substrate incubation. Along with vesicular Pgp/Pgp substrate uptake, a LysoTracker staining of neutrophils was detectable (Fig. 7*A*), thus strengthening the hypothesis that barrier bodies released by hCMEC/D3 cells and ingested by neutrophils are of lysosomal origin.

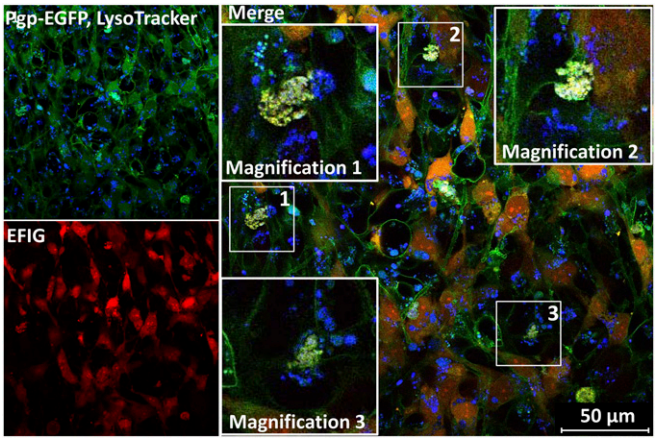

Fig. 5. Barrier bodies show lysosomal staining. Lysosomes of hCMEC/D3 cocultures were stained by incubation with 75 nM LysoTracker (blue) before EFIG-AM treatment (30 min) and subsequently analyzed via live cell imaging and confocal microscopy. Formed barrier-body aggregates, yellow in merged images (Pgp-EGFP, green; EFIG, red), additionally exhibit a blue fluorescent signal, suggesting a lysosomal origin of these structures. (*Insets*) Magnification (2.5-fold) of barrier bodies 1–3 (white frames in merged image).

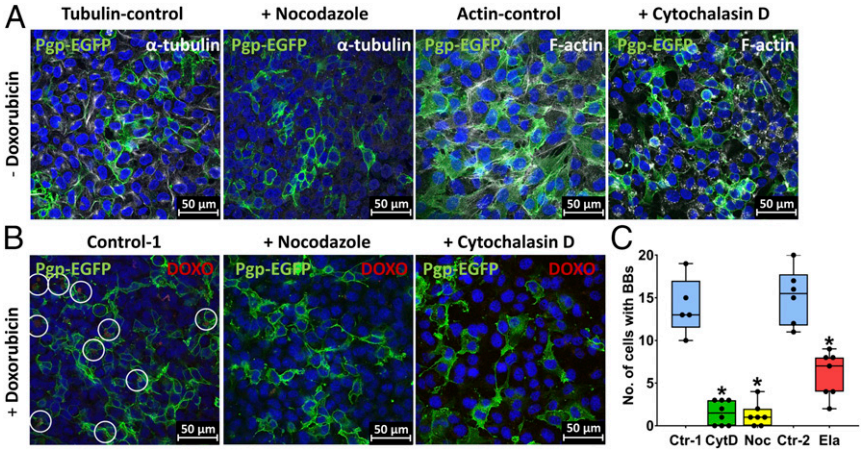

Fig. 6. Pharmacological inhibition of barrier-body formation. Effect of cytoskeleton-disrupting agents (CytD, cytochalasin D; Noc, nocodazole) and of the Pgp inhibitor elacridar (Ela) on barrier-body formation was analyzed in hCMEC/D3 cocultures. (*A*) Noc- or CytD-treated cells were analyzed with confocal fluorescence microscopy following staining of α-tubulin (white) and F-actin (white) (*Materials and Methods*). DAPI was used as nuclear counterstain (blue), and Pgp-EGFP is visualized in green. Treatment of hCMEC/D3 cultures with Noc and CytD resulted in a depolymerization of microtubules and actin filaments, respectively. (*B*) Representative images of barrier-body formation (indicated by white circles) in DOXO-treated hCMEC/D3 cultures and after incubation with Noc or CytD (*Materials and Methods*). Cells were analyzed under a confocal laser scanning microscope, and barrier-body formation was compared between treatments. (*C*) Barrier bodies and cells were counted on five or more randomly captured confocal micrographs, and a total of 785–1,008 cells were counted per treatment (for total numbers of counted cells per treatment, see *Materials and Methods*). The graph shows the number of cells with barrier bodies (BBs) per counted cells in the absence of inhibitors (Ctr-1; 8.92% of the cells exhibited barrier bodies on average) and after Noc or CytD treatment. Additionally, the graph shows the number of cells with barrier bodies per counted cells after incubation of EFIG-AM–treated cultures with Ela (*Materials and Methods*) in comparison with cultures in absence of the inhibitor (Ctr-2; 9.03% of the cells exhibited barrier bodies on average). Data are shown as boxplots with whiskers from minimum to maximum values; the horizontal line in the boxes represents the median value. In addition, individual data are shown. $*P < 0.0001$.

After addition of neutrophils to the culture medium of hCMEC/D3 cells, the neutrophils were observed to extend pseudopods directed toward the hCMEC/D3 plasma membrane (Fig. 7*B* and Movie S1, arrow 2), presumably hunting for potential target antigens. These pseudopods were not observed when neutrophils were added to hCMEC/D3 that were not exposed to DOXO or EFIG-AM and therefore did not exhibit formation of barrier bodies. Pseudopod formation by neutrophils was described as the first step in neutrophil phagocytosis (30, 31). The ingestion process of an extracellular Pgp/Pgp substrate vesicle by a nuclear-stained neutrophil is depicted in *SI Appendix*, Fig. S5. Furthermore, time-dependent uptake of barrier bodies by nuclear-stained neutrophils is shown in *SI Appendix*, Fig. S6. Control experiments showed that neutrophils cocultured with Pgp-EGFP–overexpressing cells alone (i.e., without Pgp substrate treatment) do not ingest Pgp-EGFP (*SI Appendix*, Fig. S7). Moreover, neutrophils from cocultures were analyzed by FACS for Pgp-EGFP and substrate uptake in comparison with naïve neutrophils that were not incubated with hCMECD/D3 cells. The analysis revealed that 16% of neutrophils were positive for Pgp-EGFP uptake and 69% for Pgp-substrate uptake. From Pgp-EGFP–positive cells, ∼2/3 showed a positive signal for the Pgp-substrate EFIG, resulting in a total of 11% of neutrophils that ingested both Pgp-EGFP and Pgp substrate (Fig. 7*C*). Intrinsic Pgp/Pgp-substrate vesicular uptake by neutrophils is expected to be higher, considering that endogenous unlabeled Pgp is not detectable by this fluorescence-based method. Moreover, increased substrate uptake of neutrophils might be explained by substrate release of hCMEC/D3 cells in vesicular structures and, in addition, through efflux by Pgp at the plasma membrane of hCMEC/D3 cells and subsequent uptake by neutrophils.

With respect to the timeframe of these observations, lysosomal drug sequestration and barrier-body formation could be observed after 30 min of substrate exposure of hCMEC/D3 cells. The subsequent uptake of the barrier bodies by neutrophils took place within minutes after the addition of the neutrophils to the cell culture.

To substantiate that barrier bodies are located on the apical (blood-facing) surface of endothelial cells, hCMEC/D3 cells were grown to confluency on membrane filters of two-compartment chamber devices, and neutrophils were added in the apical chamber. As shown in *SI Appendix*, Fig. S8, barrier bodies were formed at the apical plasma membrane of the endothelial cells and phagocytosed by neutrophils.

Human endothelial cells can produce interleukins (ILs) such as IL-8 (32) and the cathelicidin peptide LL-37 (33), both of which are chemotactic for neutrophils (34, 35). We therefore determined whether DOXO-treated or EFIG-AM–treated hCMEC/D3 cells produce IL-8 or LL-37. As shown in Fig. 8, cell exposure to either DOXO or EFIG-AM for 30 min significantly increased the release of IL-8, but not LL-37.

Intracellular Drug Trapping, Barrier-Body Formation, and Disposal by Neutrophils Is also Observed in Primary Cultures of Porcine BCECs. Given that hCMEC/D3 is an immortalized cell line, an alteration in its phenotype, function, and responsiveness to drugs (36) compared with the native original cell type cannot be excluded. It was therefore important to confirm that the processes observed in hCMEC/D3 cells also occur in primary BCEC cultures. For this purpose, we used porcine BCECs (pBCECs), which exhibit many similarities to human BCECs and naturally produce Pgp (37). As shown in *SI Appendix*, Fig. S9, the morphology and size of hCMEC/D3 cells and pBCECs were very similar. As reported (37), both cell types formed monolayers and showed spindle-shaped morphology when examined at confluence by phase-contrast microscopy. Pgp expression of pBCECs was similar to that of *MDR1*-EGFP–transfected hCMEC/D3 cells and significantly higher than Pgp expression of hCMEC/D3 WT cells (*SI Appendix*, Fig. S9).

Exposure of pBCEC cell cultures to subtoxic concentrations of DOXO (10 μM) led to intracellular drug trapping, barrier-body formation, and disposal by neutrophils (Fig. 9 *A* and *B*), as observed in hCMEC/D3 cells. Similarly, this process was also observed following exposure to EFIG-AM (Fig. 9*C*). Analysis of

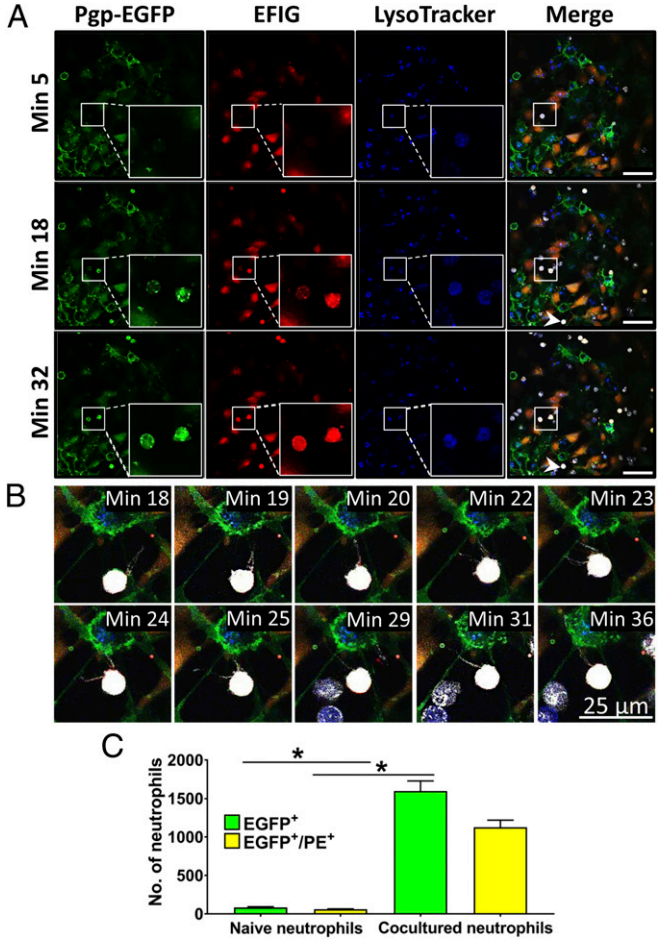

Fig. 7. Ingestion of Pgp/EFIG-enriched vesicles by neutrophils after incubation with BCECs. Cocultures of hCMEC/D3-MDR1-EGFP and hCMEC/D3 WT cells were treated with LysoTracker (blue) for visualization of lysosomes, followed by exposure to EFIG-AM (EFIG; red) and incubation with eFluor670-labeled neutrophils (white). Analysis was performed by live cell imaging using a confocal microscope at 37 °C. (*A*) Microscopy images are at indicated time points after incubation of hCMEC/D3 cell cultures with neutrophils. Uptake of Pgp/EFIG-enriched vesicles by neutrophils could be observed by increasing colocalizing punctate Pgp (green) and EFIG fluorescence signals within the neutrophils over time. Representative neutrophils, marked by white frames, are magnified (lower right). (Scale bars: 50 μm.) (*B*) Magnification of neutrophil, extending pseudopods toward the hCMEC/D3 plasma membrane, likely scanning for target antigens (same neutrophil as indicated by arrowhead in *A*). (*C*) Flow-cytometric analysis of Pgp-EGFP and EFIG uptake (PE channel) by primary neutrophils. eFluor670-labeled neutrophils were incubated for 24 h with EFIG-AM–treated hCMEC/D3 cocultures. Subsequently, uptake was compared with eFluor670-labeled control neutrophils that were not preincubated with hCMEC/D3 cells. Results are expressed as means ± SEM of three independent experiments with 10,000 measured events each. $*P < 0.05$.

the number of barrier bodies in 25 randomly captured fluorescent micrographs of different pBCEC cultures treated with either DOXO ($n = 14$) or EFIG-AM ($n = 11$) showed that 141 of 1,173 analyzed cells (12.0 ± 1.2% per image) exhibited barrier bodies without significant difference between treatments; barrier bodies were found on every single image of drug-exposed cell cultures but not in controls.

Scanning electron microscopy substantiated the budding of vesicles from the apical membrane of pBCECs after treatment with DOXO and the accumulation of the EVs in aciniform aggregates at the apical cell surface (Fig. 9*D*).

Discussion

Pgp-mediated lysosomal sequestration of cytotoxic xenobiotics such as DOXO has been shown in cancer cells (13) and peripheral organs such as kidney and spleen (14). The present experiments demonstrate that lysosomal trapping of Pgp substrates also occurs in BCECs. More importantly, we show that the intracellular Pgp-substrate–sequestering vesicular structures exit the cells and form aggregates (barrier bodies) that stay attached to the apical cell membrane of BCECs and can be phagocytosed by neutrophils, which constitutes a mechanism that might contribute to BBB protection against xenobiotic compounds (Fig. 10). The entire process of barrier-body formation could be blocked by drugs that inhibit vesicle delivery to the plasma membrane.

Why has this surprising process not been previously reported? At least three methodological prerequisites were crucial for the present observations. First, the conditional doxycycline-inducible Pgp-EGFP–expressing hCMEC/D3 cells that we recently produced (18) allowed the visualization of Pgp within and outside the BCECs. Second, the EFIG-AM uptake assay has advantages compared with the more commonly used Pgp-substrate assays because the hydrophobic, nonfluorescent EFIG-AM readily penetrates the cell membrane, where it is hydrolyzed to a hydrophilic fluorescent metabolite (EFIG) by intracellular esterases that cannot enter intracellular vesicles by passive diffusion (16). Thus, unless EFIG is actively transported out of the cell or sequestered in intracellular compartments by active transport, the esterase cleaved dye is trapped inside the cell (16). This feature thus favored the detection of Pgp-mediated lysosomal sequestration in BCECs. In this respect, EFIG differs from the more commonly used Pgp substrates, such as weakly basic chemotherapeutic agents (e.g., DOXO), which can be sequestered in lysosomes in the absence of multidrug transporters such as Pgp, most likely by pH partitioning (also referred to as ion trapping) (38–41). Third, to our knowledge, interactions between cocultures of BCECs and neutrophils have not been investigated previously for Pgp-mediated drug disposal.

According to several recent reviews, the hCMEC/D3 cell line used in our study is the most extensively characterized and used immortalized human BCEC line that is currently available as an in vitro model of the human BBB (37, 42–45). This cell line recapitulates quite effectively a considerable number of BBB–BCEC characteristics, preserving the in vivo endothelial phenotype at least until the 35th passage, including the spindle-shaped

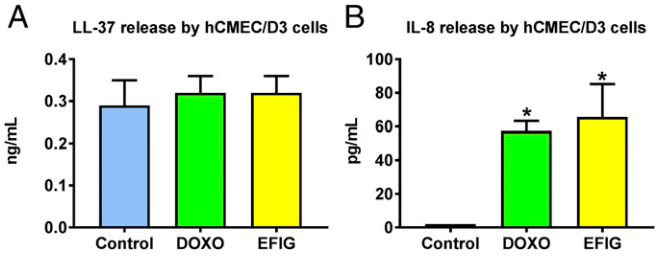

Fig. 8. Release of neutrophil-attracting chemokines by BCECs after treatment with DOXO or EFIG. hCMEC/D3-MDR1-EGFP and hCMEC/D3 WT cells were cocultured in six-well plates and treated with DOXO or EFIG-AM. The cell-culture supernatant was collected after 30 min of treatment or no treatment (control) and subjected to commercially available ELISAs to determine the specific release of neutrophil-attracting chemokines. (*A*) The release of the antimicrobial peptide LL-37 by hCMEC/D3 cells does not significantly differ between DOXO- or EFIG-treated and untreated control samples. (*B*) Levels of the neutrophil-activating peptide IL-8 are significantly elevated upon treatment with DOXO or EFIG-AM compared with untreated control samples. Values represent the mean ± SEM of identically prepared samples ($n = 6$). $*P < 0.05$.

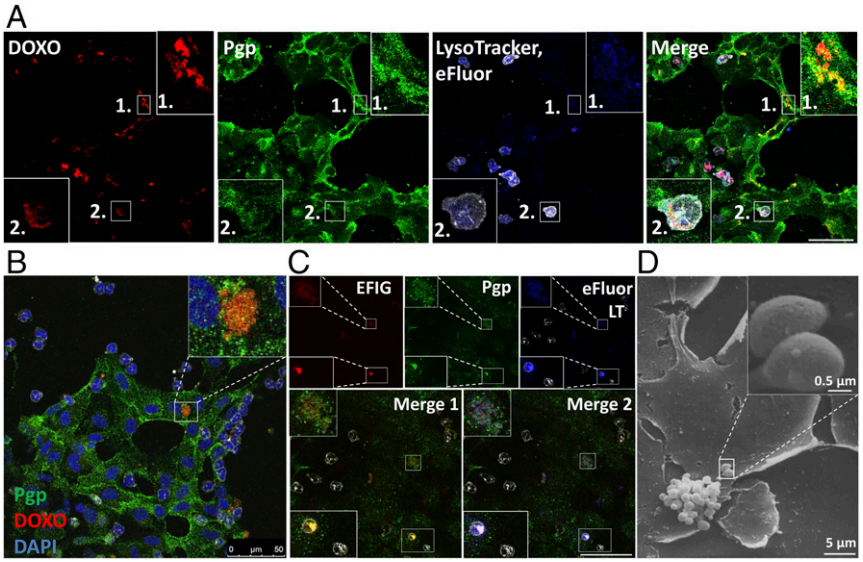

Fig. 9. Barrier-body formation and uptake by neutrophils in primary pBCEC cultures. Primary pBCECs were treated with either DOXO (10 µM, 30 min) or EFIG-AM (30 min) after culturing on collagen-coated glass coverslips for 5 d. Depending on the experiment, DOXO- or EFIG-treated cells were incubated with freshly isolated porcine neutrophils. Barrier-body formation and uptake by neutrophils were analyzed. (*A*) LysoTracker- and DOXO-treated pBCECs were incubated with eFluor670-labeled porcine neutrophils (white) for 20 min at 37 °C. Cells were fixed with aceton-methanol and indirectly stained for Pgp (*Materials and Methods*). Samples were analyzed by confocal fluorescence microscopy. Lysosomal sequestration of DOXO (1) and neutrophils exhibiting green (Pgp), red (DOXO), and blue (LysoTracker) fluorescence (2) indicate formation and phagocytosis of barrier bodies also in pBCECs. (Scale bar: 50 µm.) (*B*) Confocal fluorescence micrograph of barrier-body formation (boxed magnification) in DOXO-treated pBCECs. After DOXO treatment, cells were incubated with neutrophils for 5 min followed, by aceton-methanol fixation and indirect staining for Pgp (green). Nuclei were counterstained with DAPI (blue). (*C*) Similar to DOXO-treated pBCECs, barrier-body formation and uptake by porcine neutrophils (eFluor670-labeled, white) can be observed after treatment of the culture with EFIG (red). Cells were stained with LysoTracker (blue); Pgp (green) was indirectly stained. The overlay of Pgp, EFIG, and eFluor670 (*Inset* 1) shows colocalization of neutrophils with Pgp and EFIG substrate, as well as LysoTracker (*Inset* 2), indicating uptake of barrier bodies by neutrophils. *Insets* in the upper left and lower left show magnification of Pgp-, EFIG-, and LysoTracker-positive barrier bodies at the surface of pBCECs, as well as neutrophils. (*D*) Scanning electron micrograph of a barrier-body aggregate on the surface of a primary pBCEC after treatment with DOXO.

morphology of BCECs and the expression and topographical distribution of a number of tight junction proteins and BCEC transporters and receptors, which rendered hCMEC/D3 cells feasible for routine use (37, 42, 45). However, as shown by Urich et al. (46), compared with freshly isolated BCECs, the expression of several key protein classes, such as tight junction proteins, transporters, and cell-surface receptors, is dramatically reduced in hCMEC/D3 cells, which likely explains their low transcellular electric resistance and paracellular leakiness that decrease their usefulness as a model of the BBB. Expression of Pgp by hCMEC/D3 WT cells (compare *SI Appendix*, Fig. S9*C*) is orders of magnitude lower than that described for brain capillaries from humans (47), which was one reason to transfect these cells with human *MDR1* (15, 18). Another potential limitation of hCMEC/D3 cells relates to their origin from pathologically altered tissue (48), and it is unclear how this affects their cell biology. Human tissue is difficult to obtain on a regular basis, which has limited the development of primary cultures of human BCECs (37). Primary cultures of pBCECs form tight endothelial monolayers with a high transendothelial resistance and are suited for investigations of small-molecule transport through the BBB (37). A recent quantitative proteomics comparison of isolated brain capillaries showed that endothelial cells from porcine brain capillaries express a range of BBB-phenotype ABC transporters, with an expression closer to that of monkey and human than shown by rodent brain capillaries (49). This prompted us to evaluate whether lysosomal drug trapping, formation of barrier bodies, and disposal by neutrophils as observed in hCMEC/D3 cells also occurs in primary cultures of pBCECs. As shown here, all these processes were observed in pBCECs, including phagocytosis of barrier bodies by porcine neutrophils. Thus, with the above-described limitations of hCMEC/D3 cells in mind, the present and previous data (15, 18) indicate that *MDR1*-EGFP–transfected hCMEC/D3 cells can be used as a tool for studying principal mechanisms of drug uptake, intracellular sequestration, trafficking, and extrusion, which then have to be confirmed by primary BCEC cultures and, ultimately, in the BBB in vivo.

Neutrophils are white blood cells that act as early cellular participants in acute cerebral inflammation (50, 51). The inflammatory state causes activation of cerebral endothelial cells, leading to the adhesion and transmigration of neutrophils through the endothelial barrier to tissue sites of inflammation. In the absence of inflammatory processes, neutrophils applied to BCECs reduced BBB permeability, which was demonstrated in hCMEC/D3 cells through clearance of fluorescein isothiocyanate-labeled dextran and was also observed in vivo (52). Subsequent experiments, using the same in vitro system with hCMEC/D3 cells, showed that neutrophils block permeability increases induced by oxygen glucose deprivation (53).

If neutrophils are activated, they change shape and become more amorphous or amoeboid and can extend pseudopods by which they actively scan and probe the surroundings while they hunt for antigens (51). Neutrophils are phagocytes, capable of ingesting microorganisms or solid particles (54). Phagocytosis is a rapid process, in which neutrophils engulf particles in a target- and size-dependent manner within minutes after exposure (55–57). For neutrophil adhesion to endothelial cells during inflammation, endothelial cells produce adhesion molecules on their luminal side: the P- and E-selectins and several members of the integrin superfamily (31). Furthermore, the cytokines IL-8 and tumor necrosis factor-α and the cathelicidin peptide LL-37, which are chemotactic for neutrophils (34, 35, 58, 59), can be produced by human endothelial cells (32, 33, 60). Indeed, release of IL-8 by drug-exposed hCMEC/D3 cells was observed in the present experiments and would be a likely mechanism to explain neutrophil adhesion to

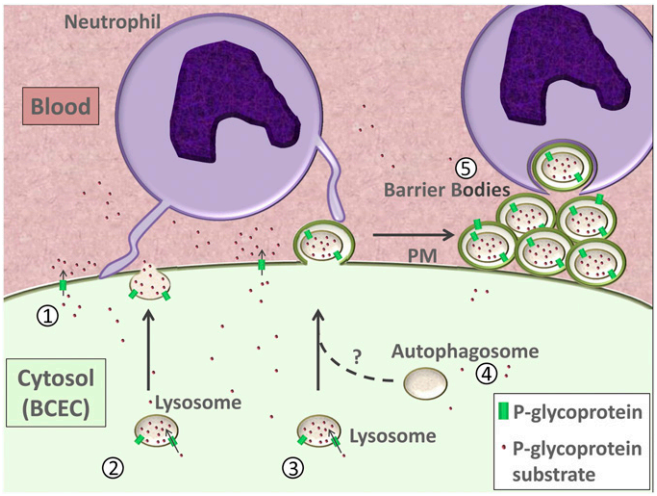

Fig. 10. Hypothesized mechanism of barrier-body formation by brain endothelial cells and disposal by neutrophils. Depicted are different mechanisms of cytoprotection against potentially cytotoxic Pgp substrates by BCECs. Cellular damage of BCECs by cytotoxic substances that are substrates for Pgp can be prevented by active efflux of substances into the extracellular space/blood via Pgp in the BCEC plasma membrane (1) or by sequestration of substrate into Pgp-enriched lysosomes that may release their content into the extracellular space via lysosomal exocytosis (2) (68). Another mechanism (described here) is the formation of Pgp/Pgp substrate-containing vesicles of lysosomal origin at the BCEC plasma membranes. The lysosome-based structures containing Pgp and Pgp substrate are released to the extracellular space via budding from the BCEC plasma membrane in an ectosome-like manner (3). Alternatively, lysosomes may fuse with autophagosomes, leading to autolysosomes (4). The autolysosomes or the vesicles of endo-lysosomal origin are released by subsequent outward budding or protrusion of the plasma membrane and form aggregates termed barrier bodies here (5). Barrier bodies are subsequently phagocytosed by neutrophils (5). Note that the different cell and vesicle types are not drawn to scale. PM, plasma membrane.

endothelial cells observed here. However, to understand molecular mechanisms by which neutrophils recognize barrier bodies, detailed proteomics of the vesicle contents provides a promising strategy to inhibit this mechanism and reverse Pgp-mediated drug resistance through barrier-body production.

Interestingly, pseudopod formation of neutrophils was also observed here and typically preceded the phagocytosis of barrier bodies. Neutrophils have no endogenous Pgp (28, 29), so phagocytosis would be the only likely mechanism by which Pgp substrates (and Pgp-EGFP) are taken up by these cells as observed here. Following phagocytosis of particles by neutrophils, the phagosome fuses with lysosomes, leading to acidification of the phagosome and degradation of the target (54).

Fig. 10 schematically illustrates the potential steps in neutrophil-mediated disposal of xenobiotics from BBB cells. In addition, known processes of Pgp-mediated drug efflux and lysosomal sequestration are shown. An open question is how the Pgp-EGFP/substrate complex that is trapped in intracellular lysosomes can undergo shedding and formation of barrier bodies. The barrier bodies observed in this study are attached to the apical cell membrane of the endothelial cells and consist of a vesicular aggregate with an aciniform structure and a size of 5–25 μm in diameter. The Pgp and Pgp substrate-containing vesicles in the barrier bodies have a diameter of 0.5–2.0 μm and contain lysosomal markers. The barrier bodies are not a nonphysiological phenomenon (or artifact) occurring only in Pgp-EGFP–transfected hCMEC/D3 cells, but they also occurred in WT hCMEC/D3 cells that received Pgp-EGFP from donor cells and in primary cultures of pBCECs. Although the exact origin of and mechanisms involved in barrier-body formation have to be clarified in more detail in future studies, the present observations allow a number of conclusions that are discussed in the following.

Multiple cell types, including endothelial cells, shed numerous, distinct forms of EVs—membrane-enclosed structures released from the cell during both physiologic and disease state (61–65). EVs are structures of variable size (from 30 nm to a few micrometers), surrounded by a lipid bilayer. Despite growing understanding of EV biogenesis, function, and contents, mechanisms regulating cargo delivery and enrichment remain largely unknown. However, the significance of EVs is expanding, as their capacity to package and transfer bioactive molecules and serve as vectors in the trafficking of cellular cargo, including chemotherapeutic drugs, is of mounting interest (64, 66).

Recent literature broadly divides cell-derived EVs into three main groups according to their biogenesis, size, and molecular composition: (*i*) exosomes (~30–100 nm in diameter), (*ii*) ectosomes (also termed microvesicles, shedded vesicles, or microparticles; ~100–1,000 nm in diameter), and (*iii*) apoptotic bodies (~1,000–5,000 nm in diameter) (63). Exosomes originate from exocytosis of multivesicular bodies (MVBs) formed by inward budding of endosomal membranes. The typically larger ectosomes originate from direct outward budding of the cellular plasma membrane. Apoptotic bodies are released by membrane blebbing of dying cells and may contain DNA and histones. Ectosomes were long considered to be artifacts, and then they were confused with exosomes—the vesicles discharged upon exocytosis of MVBs—and with cytoplasmic particles generated during apoptosis (67). EVs can be released from nearly all cell types, constitutively and/or upon induction (64), such as the EVs that sequestered Pgp substrates and formed barrier bodies after exposing the BCECs to xenobiotics like EFIG-AM or DOXO in the present study. However, at first glance, the EVs that led to barrier-body formation do not fit into the three main groups of EVs described above.

As indicated by 2 in Fig. 10, lysosomes may release their content into the extracellular space via an exocytic pathway, which has been shown to be involved in resistance to chemotherapeutic agents (13, 68); however, to our knowledge, shedding or outward budding of lysosomes has not been described, although lysosomes are able to fuse with the plasma membrane (68).

Could MVB formation play a role in the present observations? MVB formation occurs when a portion of the limiting membrane of an endosome invaginates and buds into its own lumen (69). MVBs can fuse with the cellular plasma membrane to release their intraluminal vesicles as exosomes to the extracellular space by an exocytic step (67, 70). Alternatively, MVBs can fuse with lysosomes, leading to degradation of the intraluminal vesicles and their content (54). However, exosomes (released from MVBs) are an unlikely source of barrier-body formation because they are much smaller than the EVs that formed the barrier bodies and do not contain lysosomal markers. Also, exosome isolation would require a much higher centrifugation force than that used for isolation of single barrier-body vesicles here.

Apoptotic bodies as a source of barrier-body formation could be excluded. Such apoptotic bodies are one type of EVs that contain complex cargo, both in their lumen and the lipid membrane (65). The cargo of EVs (e.g., proteins, nucleic acids, and lipids) is reflective of their cellular origin. Apoptotic bodies may contain cellular DNA as a cargo, which was not detected in barrier bodies.

Ectosomes, small plasma membrane-derived vesicles that are released by membrane blebbing from various cell types, including endothelial cells, can either fuse with target cells, with the ensuing incorporation of their membrane in the plasma membrane and release of the segregated package to the cytosol, or be taken up by endocytosis (65–67). The fate of the latter is variable: fusion with lysosomes, release of contents in the cytosol, or discharge to the extracellular space by transcytosis (67). Thus, in principle, the EVs that formed the barrier bodies in our experiments

could be a type of ectosomes (or microvesicles) that enclosed Pgp-EGFP/substrate-containing vesicles of endo-lysosomal origin (3 in Fig. 10). Indeed, transfer of Pgp by ectosomes has been shown (67), and at least part of the intercellular transfer of Pgp-EGFP between donor and recipient hCMEC/D3 cells reported by us previously was mediated by ectosomes (15). Furthermore, ectosomes have been found to sequester chemotherapeutic drugs such as DOXO (71). However, it is not clear whether ectosomes can leave the cell as such once they have entered the cell and fused with lysosomes.

Another conceivable pathway for the cargo delivery observed in this study, indicated by 4 in Fig. 10, would be fusion of lysosomes with autophagosomes (or amphisomes), leading to autolysosomes (70, 72). Autophagy is a lysosomal degradation pathway for cytoplasmic components, and increasing evidence suggests that both autophagy and lysosomal drug sequestration play a role in acquired resistance to DOXO in cancer cells (41, 73). The autolysosomes or the vesicles of endo-lysosomal origin are released by subsequent outward budding or protrusion of the plasma membrane, which might explain enclosure of barrier-body vesicles by a Pgp-containing plasma membrane.

In addition, to serve the disposal of substances that may be harmful to the cell, EVs can induce the horizontal transfer of critical molecules such as Pgp, which confers multidrug resistance to the recipient cell, as recently shown by us for Pgp-EGFP–transfected and WT hCMEC/D3 cells (15). Overall, classification of membrane vesicles, molecular details of vesicular release, clearance, and biological functions are still under intense investigation. The present description of a function of such vesicles—extracellular delivery of xenobiotics to phagocytosis by neutrophils—significantly adds to the complexity of EVs.

In addition to Pgp, other ABC transporters such as multidrug resistance protein 1 (MRP1; ABCC1) and breast cancer resistance protein (BCRP; ABCG2) can be expressed by lysosomes and mediate lysosomal drug sequestration (8, 13). Both DOXO and EFIG are not only substrates of Pgp, but also of BCRP and MRP (2, 16), which may add to the lysosomal drug sequestration observed in the present experiments, although the colocalization of Pgp-EGFP and EFIG as well as DOXO in both lysosomal vesicles and barrier bodies indicates that the sequestration was mainly mediated by Pgp. Unfortunately, the lack of inhibitors that are highly selective for only Pgp, BCRP, or MRP1 does not allow us to determine if BCRP or MRP1 added to the effect of Pgp-EGFP. For instance, verapamil, which was used by Rajagopal and Simon (8) to block MRP1 function when studying lysosomal sequestration of DOXO, also blocks Pgp, and valspodar and elacridar, which were used by Yamagishi et al. (9) to inhibit Pgp when studying lysosomal sequestration of DOXO, also block MRP1 or BCRP at higher concentrations, respectively (74). In the present experiments, elacridar inhibited barrier-body formation by ~50% when added at its IC_{50} for Pgp (0.2 μM) (75), thus substantiating the involvement of Pgp in this process.

Finally, some potential caveats need to be discussed. First, the present study utilizes a cell line (hCMEC/D3) that was transfected with a doxycycline-inducible *MDR1*-EGFP fusion plasmid, leading to a marked increase (~15-fold) in Pgp-EGFP fusion protein expression in the presence of doxycycline (18). One may argue that results obtained with such cells that highly overexpress Pgp do not relate to cells with physiological expression of Pgp. However, as discussed above, lysosomal trapping of Pgp substrates and formation of barrier bodies also occurred in WT cells that received Pgp-EGFP from donor cells, which argues against Pgp overexpression being responsible for our observations. Furthermore, intracellular trapping of Pgp substrates and formation of barrier bodies was also observed in primary cultures of pBCECs. Second, Pgp is not required for DOXO to be taken up by the lysosomes, but weak bases such as DOXO may end up in acidic compartments by simple diffusion (13, 39). However, as described above, in several cancer cell lines, lysosomal trapping of DOXO can be inhibited by blocking Pgp (9, 11–13). Furthermore, in contrast to DOXO, the hydrophilic EFIG-AM metabolite EFIG cannot enter lysosomes (or other vesicles) by passive diffusion, but only by active transport (16), which was an important reason to use this Pgp substrate in the present experiments. Third, the in vivo relevance of what is observed here remains unknown at this stage. Demonstration of these processes in vivo will be a challenging task that should be addressed in forthcoming experiments. One strategy that can be used for such experiments is positron emission tomography with radiolabeled Pgp substrates, as described by Kannan et al. (14).

In conclusion, during in vitro experiments on intercellular transfer of Pgp, we serendipitously discovered an effective cargo process for xenobiotics in human and pBCECs that involves an interaction between endothelium and neutrophils. It remains to be studied whether this cargo process only occurs at BCECs that form the BBB or also exists in other types of endothelial cells or even nonendothelial cells. As shown here, the mechanism affects a widely used chemotherapeutic drug, thus likely reducing the potential of this drug in the treatment of brain cancer. We assume that lysosomal drug sequestration and subsequent barrier-body formation and disposal via phagocytosis by neutrophils form a secondary defense mechanism if Pgp-mediated active efflux at the plasma membrane is saturated or insufficient. Continuing to uncover drug sequestration and removal in BCECs has the potential to radically change the way that we facilitate drug penetration across the BBB in the treatment of brain diseases.

Materials and Methods

The hCMEC/D3 cell line was provided by Pierre-Oliver Couraud, Institute Cochin, Paris, and stably transfected with a doxycycline-inducible *MDR1*-EGFP fusion plasmid, resulting in high expression of Pgp-EGFP fusion protein as described (18). For a heterogeneous BBB phenotype, hCMEC/D3 WT cells (8×10^5) were cocultured to equal amounts with hCMEC/D3-MDR1-EGFP cells (8×10^5), as described (15). For isolation of human blood-derived neutrophils, all subjects gave informed consent for blood sampling and analyses, and respective experiments were approved by the Ethics Committee (agreement 3295-2016) of the Hannover Medical School. Primary cultures of pBCECs and porcine neutrophils were prepared as described (76, 77). All experiments with human or porcine cell cultures were performed after cells reached confluency. See *SI Appendix, SI Materials and Methods* for full details of all experimental procedures.

ACKNOWLEDGMENTS. We thank Drs. Piet Borst, Michael M. Gottesman, Gert Fricker, and Björn Bauer for valuable comments during the final revision of the manuscript; Drs. N. Joan Abbott, Sylvia Wagner, Julia Stab, Martina Gramer, and Kerstin Römermann for help during establishing the porcine brain endothelial cell model; and Kerstin Rohn and Annika Lehmbecker for technical assistance during the electron microscopic analyses. The study was supported by Deutsche Forschungsgemeinschaft Grant LO 274/16-1.

1. Abbott NJ, Patabendige AA, Dolman DE, Yusof SR, Begley DJ (2010) Structure and function of the blood-brain barrier. *Neurobiol Dis* 37:13–25.
2. Löscher W, Potschka H (2005) Role of drug efflux transporters in the brain for drug disposition and treatment of brain diseases. *Prog Neurobiol* 76:22–76.
3. Löscher W, Potschka H (2005) Drug resistance in brain diseases and the role of drug efflux transporters. *Nat Rev Neurosci* 6:591–602.
4. Miller DS (2015) Regulation of ABC transporters blood-brain barrier: The good, the bad, and the ugly. *Adv Cancer Res* 125:43–70.
5. Fu D (2013) Where is it and how does it get there–Intracellular localization and traffic of P-glycoprotein. *Front Oncol* 3:321.
6. Ferrao P, Sincock P, Cole S, Ashman L (2001) Intracellular P-gp contributes to functional drug efflux and resistance in acute myeloid leukaemia. *Leuk Res* 25:395–405.
7. Molinari A, et al. (2002) Subcellular detection and localization of the drug transporter P-glycoprotein in cultured tumor cells. *Curr Protein Pept Sci* 3:653–670.
8. Rajagopal A, Simon SM (2003) Subcellular localization and activity of multidrug resistance proteins. *Mol Biol Cell* 14:3389–3399.

9. Yamagishi T, et al. (2013) P-glycoprotein mediates drug resistance via a novel mechanism involving lysosomal sequestration. *J Biol Chem* 288:31761–31771.
10. Gorden BH, Saha J, Khammanivong A, Schwartz GK, Dickerson EB (2014) Lysosomal drug sequestration as a mechanism of drug resistance in vascular sarcoma cells marked by high CSF-1R expression. *Vasc Cell* 6:20.
11. Seebacher NA, Lane DJ, Jansson PJ, Richardson DR (2016) Glucose modulation induces lysosome formation and increases lysosomotropic drug sequestration via the P-glycoprotein drug transporter. *J Biol Chem* 291:3796–3820.
12. Seebacher N, Lane DJ, Richardson DR, Jansson PJ (2016) Turning the gun on cancer: Utilizing lysosomal P-glycoprotein as a new strategy to overcome multi-drug resistance. *Free Radic Biol Med* 96:432–445.
13. Zhitomirsky B, Assaraf YG (2016) Lysosomes as mediators of drug resistance in cancer. *Drug Resist Updat* 24:23–33.
14. Kannan P, et al. (2011) Lysosomal trapping of a radiolabeled substrate of P-glycoprotein as a mechanism for signal amplification in PET. *Proc Natl Acad Sci USA* 108:2593–2598.
15. Noack A, Noack S, Buettner M, Naim HY, Löscher W (2016) Intercellular transfer of P-glycoprotein in human blood-brain barrier endothelial cells is increased by histone deacetylase inhibitors. *Sci Rep* 6:29253.
16. Lebedeva IV, Pande P, Patton WF (2011) Sensitive and specific fluorescent probes for functional analysis of the three major types of mammalian ABC transporters. *PLoS One* 6:e22429.
17. Huber O, et al. (2012) Localization microscopy (SPDM) reveals clustered formations of P-glycoprotein in a human blood-brain barrier model. *PLoS One* 7:e44776.
18. Noack A, et al. (2014) Drug-induced trafficking of p-glycoprotein in human brain capillary endothelial cells as demonstrated by exposure to mitomycin C. *PLoS One* 9: e88154.
19. Mahoney BP, Raghunand N, Baggett B, Gillies RJ (2003) Tumor acidity, ion trapping and chemotherapeutics. I. Acid pH affects the distribution of chemotherapeutic agents in vitro. *Biochem Pharmacol* 66:1207–1218.
20. Akers JC, Gonda D, Kim R, Carter BS, Chen CC (2013) Biogenesis of extracellular vesicles (EV): Exosomes, microvesicles, retrovirus-like vesicles, and apoptotic bodies. *J Neurooncol* 113:1–11.
21. Huang-Doran I, Zhang CY, Vidal-Puig A (2017) Extracellular vesicles: Novel mediators of cell communication in metabolic disease. *Trends Endocrinol Metab* 28:3–18.
22. Kreft M, Potokar M, Stenovec M, Pangrsic T, Zorec R (2009) Regulated exocytosis and vesicle trafficking in astrocytes. *Ann N Y Acad Sci* 1152:30–42.
23. Mazel T (2017) Crosstalk of cell polarity signaling pathways. *Protoplasma* 254: 1241–1258.
24. Breitfeld PP, McKinnon WC, Mostov KE (1990) Effect of nocodazole on vesicular traffic to the apical and basolateral surfaces of polarized MDCK cells. *J Cell Biol* 111: 2365–2373.
25. Arnette C, Frye K, Kaverina I (2016) Microtubule and actin interplay drive intracellular c-Src trafficking. *PLoS One* 11:e0148996.
26. Tajika Y, et al. (2005) Differential regulation of AQP2 trafficking in endosomes by microtubules and actin filaments. *Histochem Cell Biol* 124:1–12.
27. Jacob C, et al. (2002) DMSO-treated HL60 cells: A model of neutrophil-like cells mainly expressing PDE4B subtype. *Int Immunopharmacol* 2:1647–1656.
28. Ben-Chetrit E, Levy M (1998) Does the lack of the P-glycoprotein efflux pump in neutrophils explain the efficacy of colchicine in familial Mediterranean fever and other inflammatory diseases? *Med Hypotheses* 51:377–380.
29. Lu MC, et al. (2008) Increased multidrug resistance-associated protein activity in mononuclear cells of patients with systemic lupus erythematosus. *Clin Exp Rheumatol* 26:638–645.
30. Dale DC (2009) Neutrophil biology and the next generation of myeloid growth factors. *J Natl Compr Canc Netw* 7:92–98.
31. Amulic B, Cazalet C, Hayes GL, Metzler KD, Zychlinsky A (2012) Neutrophil function: From mechanisms to disease. *Annu Rev Immunol* 30:459–489.
32. Stanimirovic D, Satoh K (2000) Inflammatory mediators of cerebral endothelium: A role in ischemic brain inflammation. *Brain Pathol* 10:113–126.
33. Edfeldt K, et al. (2006) Involvement of the antimicrobial peptide LL-37 in human atherosclerosis. *Arterioscler Thromb Vasc Biol* 26:1551–1557.
34. Verjans ET, Zels S, Luyten W, Landuyt B, Schoofs L (2016) Molecular mechanisms of LL-37-induced receptor activation: An overview. *Peptides* 85:16–26.
35. Zeilhofer HU, Schorr W (2000) Role of interleukin-8 in neutrophil signaling. *Curr Opin Hematol* 7:178–182.
36. Kaur G, Dufour JM (2012) Cell lines: Valuable tools or useless artifacts. *Spermatogenesis* 2:1–5.
37. Helms HC, et al. (2016) In vitro models of the blood-brain barrier: An overview of commonly used brain endothelial cell culture models and guidelines for their use. *J Cereb Blood Flow Metab* 36:862–890.
38. Jaffrézou JP, Levade T, Chatelain P, Laurent G (1992) Modulation of subcellular distribution of doxorubicin in multidrug-resistant P388/ADR mouse leukemia cells by the chemosensitizer ((2-isopropyl-1-(4-[3-N-methyl-N-(3,4-dimethoxy-beta- phenethyl) amino]propyloxy)-benzenesulfonyl))indolizine. *Cancer Res* 52:6440–6446.
39. Larsen AK, Escargueil AE, Skladanowski A (2000) Resistance mechanisms associated with altered intracellular distribution of anticancer agents. *Pharmacol Ther* 85: 217–229.
40. Duvvuri M, Konkar S, Funk RS, Krise JM, Krise JP (2005) A chemical strategy to manipulate the intracellular localization of drugs in resistant cancer cells. *Biochemistry* 44:15743–15749.
41. Guo B, Tam A, Santi SA, Parissenti AM (2016) Role of autophagy and lysosomal drug sequestration in acquired resistance to doxorubicin in MCF-7 cells. *BMC Cancer* 16:762.
42. Weksler B, Romero IA, Couraud PO (2013) The hCMEC/D3 cell line as a model of the human blood brain barrier. *Fluids Barriers CNS* 10:16.
43. Rahman NA, et al. (2016) Immortalized endothelial cell lines for in vitro blood-brain barrier models: A systematic review. *Brain Res* 1642:532–545.
44. Gameiro M, et al. (2017) Cellular models and in vitro assays for the screening of modulators of P-gp, MRP1 and BCRP. *Molecules* 22:E600.
45. Kaisar MA, et al. (2017) New experimental models of the blood-brain barrier for CNS drug discovery. *Expert Opin Drug Discov* 12:89–103.
46. Urich E, Lazic SE, Molnos J, Wells I, Freskgård PO (2012) Transcriptional profiling of human brain endothelial cells reveals key properties crucial for predictive in vitro blood-brain barrier models. *PLoS One* 7:e38149.
47. Hartz AM, et al. (2017) P-gp protein expression and transport activity in rodent seizure models and human epilepsy. *Mol Pharm* 14:999–1011.
48. Weksler BB, et al. (2005) Blood-brain barrier-specific properties of a human adult brain endothelial cell line. *FASEB J* 19:1872–1874.
49. Kubo Y, Ohtsuki S, Uchida Y, Terasaki T (2015) Quantitative determination of luminal and abluminal membrane distributions of transporters in porcine brain capillaries by plasma membrane fractionation and quantitative targeted proteomics. *J Pharm Sci* 104:3060–3068.
50. Ransohoff RM, Brown MA (2012) Innate immunity in the central nervous system. *J Clin Invest* 122:1164–1171.
51. Kolaczkowska E, Kubes P (2013) Neutrophil recruitment and function in health and inflammation. *Nat Rev Immunol* 13:159–175.
52. Joice SL, et al. (2009) Modulation of blood-brain barrier permeability by neutrophils: In vitro and in vivo studies. *Brain Res* 1298:13–23.
53. Cowan KM, Easton AS (2010) Neutrophils block permeability increases induced by oxygen glucose deprivation in a culture model of the human blood-brain barrier. *Brain Res* 1332:20–31.
54. Richards DM, Endres RG (2014) The mechanism of phagocytosis: Two stages of engulfment. *Biophys J* 107:1542–1553.
55. Lee WL, Harrison RE, Grinstein S (2003) Phagocytosis by neutrophils. *Microbes Infect* 5: 1299–1306.
56. Lee CY, Herant M, Heinrich V (2011) Target-specific mechanics of phagocytosis: Protrusive neutrophil response to zymosan differs from the uptake of antibody-tagged pathogens. *J Cell Sci* 124:1106–1114.
57. Branzk N, et al. (2014) Neutrophils sense microbe size and selectively release neutrophil extracellular traps in response to large pathogens. *Nat Immunol* 15: 1017–1025.
58. Newman I, Wilkinson PC (1989) Chemotactic activity of lymphotoxin and tumour necrosis factor alpha for human neutrophils. *Immunology* 66:318–320.
59. Dürr UH, Sudheendra US, Ramamoorthy A (2006) LL-37, the only human member of the cathelicidin family of antimicrobial peptides. *Biochim Biophys Acta* 1758: 1408–1425.
60. Kim TH, Ku SK, Lee IC, Bae JS (2012) Anti-inflammatory effects of kaempferol-3-O-sophoroside in human endothelial cells. *Inflamm Res* 61:217–224.
61. György B, et al. (2011) Membrane vesicles, current state-of-the-art: Emerging role of extracellular vesicles. *Cell Mol Life Sci* 68:2667–2688.
62. Shifrin DA, Jr, Demory Beckler M, Coffey RJ, Tyska MJ (2013) Extracellular vesicles: Communication, coercion, and conditioning. *Mol Biol Cell* 24:1253–1259.
63. Vader P, Breakefield XO, Wood MJ (2014) Extracellular vesicles: Emerging targets for cancer therapy. *Trends Mol Med* 20:385–393.
64. Ciardiello C, et al. (2016) Focus on extracellular vesicles: New frontiers of cell-to-cell communication in cancer. *Int J Mol Sci* 17:175.
65. Kalra H, Drummen GP, Mathivanan S (2016) Focus on extracellular vesicles: Introducing the next small big thing. *Int J Mol Sci* 17:170.
66. Gong J, Jaiswal R, Dalla P, Luk F, Bebawy M (2015) Microparticles in cancer: A review of recent developments and the potential for clinical application. *Semin Cell Dev Biol* 40:35–40.
67. Cocucci E, Meldolesi J (2011) Ectosomes. *Curr Biol* 21:R940–R941, and erratum (2012) 22:1359.
68. Settembre C, Ballabio A (2014) Lysosomal adaptation: How the lysosome responds to external cues. *Cold Spring Harb Perspect Biol* 6:a016907.
69. Piper RC, Katzmann DJ (2007) Biogenesis and function of multivesicular bodies. *Annu Rev Cell Dev Biol* 23:519–547.
70. Fader CM, Colombo MI (2009) Autophagy and multivesicular bodies: Two closely related partners. *Cell Death Differ* 16:70–78.
71. Gong J, et al. (2013) Microparticle drug sequestration provides a parallel pathway in the acquisition of cancer drug resistance. *Eur J Pharmacol* 721:116–125.
72. Cocucci E, Meldolesi J (2015) Ectosomes and exosomes: Shedding the confusion between extracellular vesicles. *Trends Cell Biol* 25:364–372.
73. Chen C, et al. (2018) Autophagy and doxorubicin resistance in cancer. *Anticancer Drugs* 29:1–9.
74. Wu CP, Calcagno AM, Ambudkar SV (2008) Reversal of ABC drug transporter-mediated multidrug resistance in cancer cells: Evaluation of current strategies. *Curr Mol Pharmacol* 1:93–105.
75. Kühnle M, et al. (2009) Potent and selective inhibitors of breast cancer resistance protein (ABCG2) derived from the p-glycoprotein (ABCB1) modulator tariquidar. *J Med Chem* 52:1190–1197.
76. Stab J, et al. (2017) Flurbiprofen-loaded nanoparticles can cross a primary porcine in vitro blood-brain barrier model to reduce amyloid-β 42 burden. *J Nanomed Biother Discov* 6:140.
77. de Buhr N, et al. (2017) Neutrophil extracellular trap formation in the *Streptococcus suis*-infected cerebrospinal fluid compartment. *Cell Microbiol* 19:e12649.